

# Correlation between microstructure and properties of biocomposite coatings

E. Verné\*, E. Bona, E. Angelini, F. Rosalbino, P. Appendino

Materials Science and Chemical Engineering Department, C.so Duca degli Abruzzi 24, 10129 Torino, Italy

Received 19 July 2001; received in revised form 13 December 2001; accepted 6 January 2002

## Abstract

A  $\text{SiO}_2\text{--CaO--Na}_2\text{O}$  (SCN) based bioactive glass was used to prepare glass–matrix/Ti particle composite coatings (SCNT). The coatings were obtained by vacuum plasma spray (VPS) on Ti–6Al–4V substrates. Two different deposition methods have been compared: (a) VPS of powders obtained by ball milling of sintered composites; (b) *in situ* plasma spray of mixed titanium and glass powders. For comparative purposes, pure SCN glass coatings were produced. The coating morphology and microstructure were observed by optical and scanning electron microscopy, compositional analyses by energy dispersive X-ray spectroscopy (EDS), and X-ray diffraction (XRD). Comparative mechanical tests were carried out by shear tests and by Vickers indentations at the interface between the substrate and the coatings. The bioactivity of glass- and composite coatings was investigated *in vitro* by soaking them in a simulated body fluid (SBF) with the same ion concentration of the human plasma. All the layers retain their starting composition. The composite coatings obtained by VPS of the powdered presintered composites showed a better mechanical behaviour with respect both to the composite coatings obtained by the *in situ* method and to the pure glass coatings. Both the glass- and the two kind of composite coatings revealed to be bioactive by the growth of a thick apatite layer after 30 days of soaking in SBF. The electrochemical behaviour of the SCNT coatings was evaluated by means of potentiodynamic anodic polarization curves and free corrosion potential measurements in Ringer solution at 25 °C. For comparative purposes the same analyses were performed on analogous bioactive glass–matrix/Ti particle composite coated samples, based on the system  $\text{TiO}_2\text{--SiO}_2\text{--CaO--B}_2\text{O}_3$  (TSCB), and obtained both by the *in situ* and by presintering method as well. The results of the electrochemical tests showed a better corrosion behaviour of the samples coated by VPS of powdered sintered composites with respect to those coated by *in situ* VPS composites. © 2002 Elsevier Science Ltd. All rights reserved.

**Keywords:** Bioactive coatings; Glass-matrix composites; Plasma spraying; Electrochemical properties; Coatings;  $\text{SiO}_2\text{--CaO--Na}_2\text{O}$

## 1. Introduction

The possibility of using bioactive glasses as substitutes of several parts of the skeletal system become more and more studied, because of their property of chemical bonding to the living tissues. Their bioactivity is often tested *in vitro* by observing the precipitation of an apatite layer from a simulated body fluid (SBF); *in vivo* this layer provides a strong bonding to the tissues.<sup>1,2</sup> Unfortunately, few of these bioactive glasses could be used for clinical applications as bulk materials: even if a stable interface with the tissues is guaranteed, their poor mechanical properties do not allow us to use them in load bearing devices. However, their mechanical prop-

erties could be enhanced by reinforcing them with metallic particles (obtaining bioactive glass–matrix composite materials, i.e. “biocomposites”).<sup>3</sup> These biocomposites could be prepared as bulk materials as well as coatings on tough substrates. For example, bioactive glass–matrix/Ti particle composite coatings have been successfully deposited on Ti alloy substrates<sup>4–8</sup> by vacuum plasma spray (VPS). In this case the bioactive coating provides both a chemical bonding to the bone and a tough behaviour. Moreover metallic substrates could be protected from corrosion and ion release.

The VPS technique provides adherent and dense coatings, and it is possible to control morphology, thickness, structure and properties of the coatings by tailoring the deposition parameters.

In order to produce composite coatings different methods can be used:

\* Corresponding author. Fax: +39-011-5644699.

E-mail address: verne@athena.polito.it (E. Verné).

1. VPS of “composite powders”, i.e. spraying Ti particles coated by glass, obtained by milling a bulk sintered composite;<sup>4–8</sup>
2. VPS in situ, i.e. simply mixing glass powders and titanium particles and vacuum plasma spraying the mixture on the substrates.<sup>9</sup>

In this work two bioactive glasses (SCN, TSCB),<sup>4,10</sup> were used as matrices for the preparation of 15vol% Ti particle reinforced composite coatings on sand blasted Ti–6Al–4V substrates. The coatings have been obtained by using the above-mentioned two different VPS methods. The aim of this study is to compare the microstructure, the properties and the electrochemical behaviour of the coatings provided by these two different ways.

## 2. Experimental

The glasses used in this work have the following mol% compositions: 50.0 SiO<sub>2</sub>, 25.0 CaO, 25.0 Na<sub>2</sub>O (SCN) and 46.6 SiO<sub>2</sub>, 48.7 CaO, 2.5 B<sub>2</sub>O<sub>3</sub>, 2.2 TiO<sub>2</sub> (TSCB). These two glasses were chosen because of their known bioactivity.<sup>4,10</sup> They were prepared by melting the starting products (SiO<sub>2</sub>, CaCO<sub>3</sub>, Na<sub>2</sub>CO<sub>3</sub>, TiO<sub>2</sub>, H<sub>3</sub>BO<sub>3</sub>) in a platinum crucible (Linn Elektronik 1880). The raw materials were intimately mixed and heated starting from room temperature up to the final temperature with a scan of 2000 °C/h. They were maintained at 1600–1650 °C for 1 h. The melted glasses were quenched into cold water, dried at 100 °C for 1 h, powdered in a ball mill and sieved up to a grain size of 70–100 µm. The characteristic temperatures of the two glasses were determined by means of differential thermal analysis (DTA Netzsch 404 S) and differential scanning calorimetry (Perkin Elmer DSC 7).

Part of the SCN glass was poured on a stainless steel sheet heated at 300 °C (to avoid as much as possible thermal shocks) in order to obtain bars, which were successively annealed at 450 °C for 2 h (time and temperature conditions determined on the basis of the characteristic temperatures of the glass), and polished to a final size of 50×7×3 mm<sup>3</sup>. The bars were utilised to measure density (Archimede's method), softening temperature and linear expansion coefficient (Netzsch dilatometer) of the base glass. Part of the SCN powders was then mixed with 15 vol.% of Ti particles (Plasma Technik 99,99% purity) with a mean size up to 50 µm, in order to prepare the SCNT composite.

The thermal properties of the mixture SCN glass/Ti were determined by means of differential scanning calorimetry. The linear shrinkages of the glass and glass plus Ti powders were measured between room temperature and 950–1000 °C by means of dilatometry (heating rate 10 °C/min, under Ar flow), on green com-

pacts of 50×5×3 mm<sup>3</sup> size obtained by uniaxial pressing (150 MPa load for 60 s, using ethanol as liquid binder).

A calorimetric study of the sintering process was performed, as described elsewhere,<sup>3,8,11</sup> by DSC, with the aim of preparing sintered samples with a homogeneous interface between the Ti particles and the glass–matrix. In this way, a temperature close to the softening point, in order to avoid as much as possible the crystallisation of the glass–matrix, and to induce as well a good wetting of the titanium particles by the glass–matrix, was determined. On the basis of this study, glass–ceramic matrix composites (SCNT) were prepared by pressureless sintering of the glass plus Ti green compacts at 600 °C for 2 h in Ar flow. Both the bulk glasses and the sintered composites were ball milled in an automatic mortar and sieved up to 63–100 µm. After milling, a morphological (SEM) and compositional (EDS) analysis of the powdered composite was performed, in order to check if the titanium particles were still embedded in the glass–matrix. The glass and the composite powders were then deposited by vacuum plasma spray (VPS, Plasma Technik AG, JRC Ispra-Va-Italy) on Ti–6Al–4V substrates (sheets of 10×10 mm<sup>2</sup> area, 3 mm height) previously sand blasted ( $R_a=2.5$  µm, measured by Hommel P5-R50M) and ultrasonically cleaned in acetone. Some composite coatings were also produced by the in situ method, i.e. by mixing the glass powders and the titanium particles and by vacuum plasma spraying the mixture on the substrates, without any previous sintering treatment. The VPS deposition parameters were optimised as a function of the powder composition.

The coated samples were characterised by optical and scanning electron microscopy (SEM Philips PW 1830), compositional (EDS, Philips EDAX 9100) and structural analyses (XRD, Philips PW 1710), mechanical tests (Vickers indentations at the interface between the substrate and the coating; comparative shear tests by means of a Schenck–Trabel equipment). The coated specimens (10×10 mm<sup>2</sup>) for the shear test were glued together with Araldite AV 119 (Ciba-Geigy) and cured 40 min at 120 °C, as described in the literature.<sup>12–16</sup> At least ten specimens for each sample were used for this test.

Some in vitro tests were performed in order to test the bioactivity of the coatings, by soaking samples of each coating for 30 days in 50 ml of a simulated body fluid (SBF) with the same composition of the human plasma<sup>1,2</sup> (polyethylene bottles, at 37 °C). After soaking, the samples were removed from the solution, dried at room temperature and analysed by SEM, EDS and XRD.

For comparative purposes, two sets of TSCB matrix/Ti particle composite coatings (TSCBT) were also produced, as described in Ref. 4, by vacuum plasma spraying of powdered presintered composites, and by the as described in situ method.

In order to investigate the reliability of the different composites, the electrochemical behaviour of the SCNT

and TSCBT coated samples has been evaluated by means of potentiodynamic anodic polarisation curves and free corrosion potential measurements performed in Ringer solution (NaCl 9.00 g; NaHCO<sub>3</sub> 0.20 g; KCl 0.43 g; CaCl<sub>2</sub> 0.24 g; distilled water up to 1 dm<sup>3</sup>) at room temperature. The anodic polarization curves have been recorded starting from the open circuit potential and scanning the potential in the more noble direction at a scan rate of  $2.5 \times 10^{-1}$  mV s<sup>-1</sup>. The free corrosion potential (FCP) was measured at 60 s. intervals for up to  $8 \times 10^4$  s, with respect to a saturated calomel electrode (SCE).

### 3. Results and discussion

#### 3.1. Sintering process optimisation

Table 1 reports the characteristic temperatures [glass transition temperature ( $T_g$ ), dilatometric softening temperature ( $T_{\text{soft}}$ ), crystallisation temperature ( $T_x$ ), liquidus temperature ( $T_l$ )] and some other properties (density and linear expansion coefficient) of the SCN and TSCB glasses. In order to produce the sintered SCNT composites, a suitable temperature and a time schedule were individuate. To this purpose, the above mentioned calorimetric study described in the literature<sup>3,8,10</sup> was carried out on glass and glass plus titanium powders.

The best sintering temperature is normally in the range between the glass transition temperature and the crystallisation temperature. In fact, in this range, the viscous flow typical of amorphous phases can be fully used. During the sintering condition study, the attention was also focused on the reactivity of the titanium particles towards the glass matrix, in order to avoid as much as possible any modification of its starting composition which could affect its bioactivity.<sup>17,18</sup>

#### 3.2. Sintered samples characterisation

The optimised viscous flow sintering process provided SCNT composite samples with densities close to 80% of the theoretical one. The theoretical density of SCNT composite was calculated using the mixture law, starting from Ti density (known from literature) and the density of SCN glass measured by Archimede's method on bulk specimens.

Table 1  
Characteristic temperatures, density and linear expansion coefficient of the SCN and TSCB glasses

Sample	$T_g$ (°C)	$T_{\text{soft}}$ (°C)	$T_x$ (°C)	$\Delta T_l$ (°C)	$d$ (g/cm <sup>3</sup> )	$\alpha$ (°C <sup>-1</sup> )
TSCB	740 ± 2	820 ± 2	881 ± 2	> 1200	2.91	–
SCN	543 ± 2	560 ± 2	665 ± 2	1200–1240	2.72	$16.6 \times 10^{-6}$

These samples showed a microstructure almost completely amorphous, with very few crystalline phase, as deduced by analysing the composite by XRD : only Ti peaks and some of the stronger lines of Na<sub>2</sub>Ca<sub>2</sub>(SiO<sub>3</sub>)<sub>3</sub> were visible in the amorphous background. Even if the calorimetric scan did not detect any crystallisation before 665 °C (see Table 1) the isothermal treatment at 600 °C for 2 h was long enough to induce a partial crystallisation of Na<sub>2</sub>Ca<sub>2</sub>(SiO<sub>3</sub>)<sub>3</sub>.

EDS analysis performed on the bulk glass and on the glass–matrix of the sintered composite showed that the matrix does not change its composition during the sintering process; no Ti was detected into the glass–matrix since the sintering temperature was too low to cause any detrimental reaction between the glass and the metal, but high enough to provide the metal wetting by the viscous glass and to guarantee the adhesion between the two materials. SEM and EDS analyses performed on powdered composite showed that the Ti particles were covered by a glass layer : the grinded sintered composite was a “composite powder”, and not only a mixture of Ti and glass powders.

#### 3.3. Coatings preparation and characterisation

The VPS technique provided about 150 µm thick SCN and SCNT coatings. Table 2 reports the deposition parameters chosen in this work. The interfaces, between the substrate and each kind of VPS coating are homogeneous and the coatings, are scarcely porous, as shown by Fig. 1, where a polished cross section of a SCN glass coated sample is reported.

However, the morphology of the in situ SCNT composite coatings and that of the presintered SCNT composite coatings are completely different one from each other. This feature is clearly observable in Figs. 2 and 3, respectively. The in situ composite coating (Fig. 2) is scarcely porous, but the Ti particle morphology has changed from particles to platelets, providing a layered composite structure, with a little discontinuity between the glass–matrix and the reinforcing phase. On the contrary, the presintered composite coating (Fig. 3) is more homogeneous : the Ti particles are well embedded into the glass–matrix and the cohesion degree of the whole

Table 2  
VPS deposition parameters

Parameter	Sputtering	Deposition
Mean particle size (mm)	–	63–100
Chamber pressure (MPa)	0.002	0.015–0.017
Gas flow rate (l/min)	40Ar–1.7 H <sub>2</sub>	50 Ar–1.7 H <sub>2</sub>
Current (A)	300	600
Tension (V)	60–50	60–50
Powder flow rate (g/min)	–	17
Distance to arch/substrate (mm)	105	105
Toarch angle	65°	90°

coating is likely to be higher. In this second case, the matrix seems to be partially crystallised. The compositional analysis (EDS) performed on the bulk SCN glass and on the glass–matrix of each SCNT composite coatings revealed that the SCN glass–matrix retained its starting composition in each step of the coating generation (see Table 3). The XRD analysis showed that the SCN glass coating and the in situ SCNT composite coatings are still amorphous (only Ti peaks are evident in the amorphous background in the in situ SCNT pattern), while the presintered SCNT composite coating shows that a small amount of the crystalline phase  $\text{Na}_2\text{Ca}_2(\text{SiO}_3)_3$ , is present (Fig. 4). This phase is likely to be formed during the presintering process, since it was individuated by XRD analyses on the sintered composite, before the VPS deposition.

### 3.4. Mechanical tests

Several Vickers indentations, with different loads up to 10 N, were produced at the interface between the

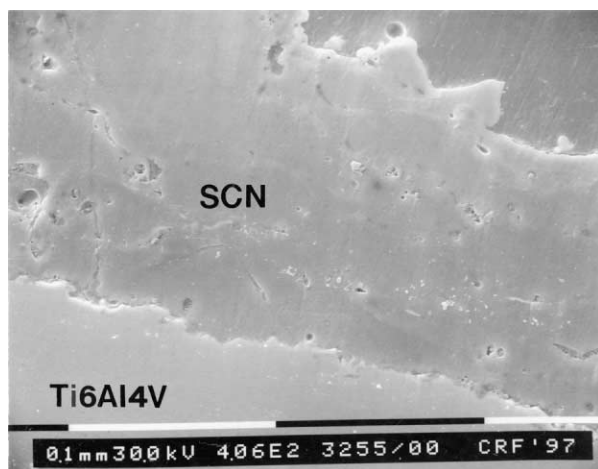


Fig. 1. Polished cross section of a SCN glass coated sample.

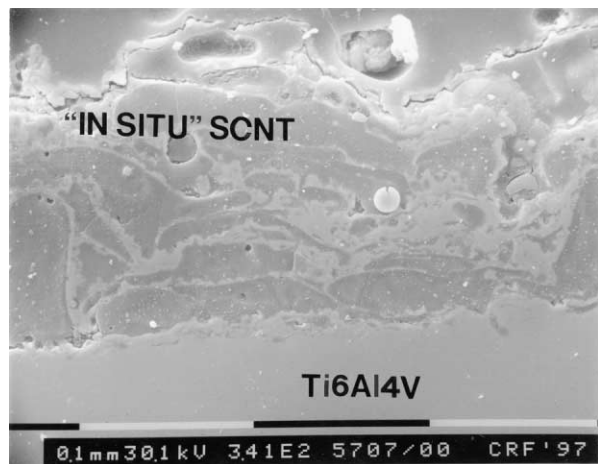


Fig. 2. Polished cross section of an in situ SCNT composite coating.

substrate and the coatings with the aim of studying qualitatively the induced crack propagation in the glass or composite coatings.<sup>19</sup> The samples showed in Fig. 5a and b have been indented with a 5 N load. The in situ SCNT coating (Fig. 5a) revealed a crack propagation parallel to the interface between the coating and the substrate and at the interface between the glass–matrix and the metal platelets (see arrows). On the contrary, the indentation at the interface between the presintered SCNT composite coating and the substrate (Fig. 5b) produced some crack in different directions being partially deviated by the Ti particles and by the few  $\text{Na}_2\text{Ca}_2(\text{SiO}_2)_3$  crystals (see arrows), but no cracks propagated at the interface between the matrix and the Ti particles nor parallel to the coating/substrate interface, and no glass/metal interface detaching was observed. Only in this second case, the Ti particles seems to have a complete role of fracture energy consumers. A 10 N load caused a similar behaviour in the presintered composite coating, but a dramatic failure in the in situ one. The crack propagation path was different in the in situ coatings in respect to the presintered ones, because of the different morphology and geometry of titanium inclusions.

In the case of the SCN glass coatings (not reported here), the indentation induced some cracks both parallel and orthogonal to the interface with the substrate, and the coating failed at very low indentation loads (less than 5 N).

The adherence of the SCN and the two SCNT coatings to the substrate was comparatively evaluated by means of shear tests. The results for the coatings showed in this work are summarised in Table 4. The presintered SCNT coatings, demonstrated a better mechanical behaviour and less data dispersion in comparison both to the in situ SCNT coatings and to the pure SCN coatings. Moreover, these values are in agreement or higher than those obtained for analogous

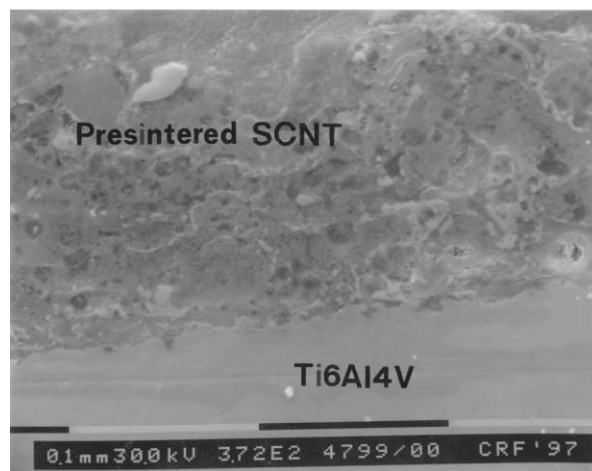


Fig. 3. Polished cross section of a presintered SCNT composite coating.

Table 3

EDS results of the analyses performed on the SCN glass matrix at different process steps (wt.% of the elements)<sup>a</sup>

Element	SCN bulk	In situ SCNT matrix	Presintered SCNT matrix
Si	44.9	44.4	45.2
Ca	38.9	38.8	38.4
Na	16.2	16.8	16.4

<sup>a</sup> EDS results are reported as semi-quantitative data, for comparative purposes. They are not comparable with the theoretical mol% of the oxides in the starting glass-matrix.

VPS coatings tested in similar conditions.<sup>3</sup> A morphological observation performed on the specimens after mechanical tests revealed a cohesive failure in the presintered composite coatings and an adhesive one on both the in situ composite coatings and the pure SCN coatings. This feature is in agreement with the different crack propagation path evidenced in the two composites by Vickers indentation. The different failure mechanism is likely to be related to the more homogeneous structure of the presintered composite coatings in comparison to the other ones.

### 3.5. *In vitro* tests

Fig. 6 shows the plan view of a presintered SCNT composite coating after 30 days soaking in SBF. The coating is covered by a thick self-grown apatite layer with the typical spheroidal morphology and some

cracks due to the drying process. The EDS analysis performed on this layer revealed the presence of Si, Ca and P ions, with a Ca/P weight ratio close to the theoretical value for apatite (i.e. 2.15). The same layer was observed on the in situ composite coatings and on the pure glass coatings. Fig. 7 shows the XRD patterns of the SCN, the in situ SCNT and the presintered SCNT coatings respectively after 30 days soaking in SBF. It is evident the presence of the strongest signals of apatite in all the patterns. These *in vitro* tests proved that both the glass and the composite coatings are still bioactive. The bioactivity of the bulk SCN is well known;<sup>10</sup> the addition of Ti particles in the composite did not reduce its bioactivity in terms of the formation of an apatite layer.

### 3.6. *Electrochemical characterisation*

The TSCBT sintered composites and the TSCBT VPS coatings have been characterised from a morphological, structural and compositional point of view (SEM, EDS, XRD) as described in Refs. 4 and 6. Their bioactivity was also demonstrated by soaking them in SBF.<sup>4</sup> In this work, only the electrochemical behaviour of the presintered and of the in situ TSCBT coatings will be commented on, in order to compare it with that of the SCNT composite coatings.

Fig. 8 shows the anodic polarization curves recorded in Ringer's solution on SCNT coated samples. No active-passive transition is observed in the case of presintered SCNT coating which exhibits only a limiting

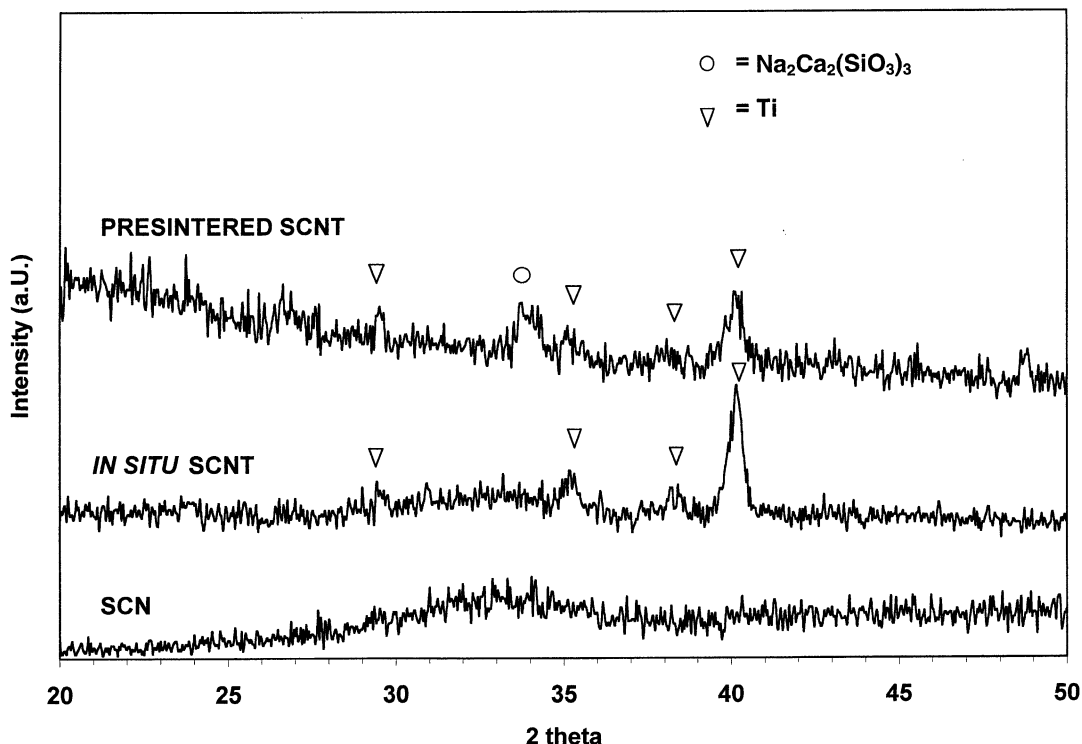
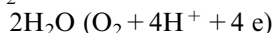


Fig. 4. XRD patterns of SCN and SCNT VPS coatings.

current density ( $0.3 \text{ mA/cm}^2$ ) in a wide potential range [between 2500 and 6500 mV(SCE)]; on the contrary the in situ SCNT coating shows a very high critical passivating current density ( $6 \text{ mA/cm}^2$ ) with a passive range between 3500 and 6500 V(SCE) characterised by a current density plateau of  $1.5 \text{ mA/cm}^2$ . In both cases the increase of the current density, observed for potential values higher than 6500 mV(SCE), is attributable to the  $\text{O}_2$  evolution reaction:



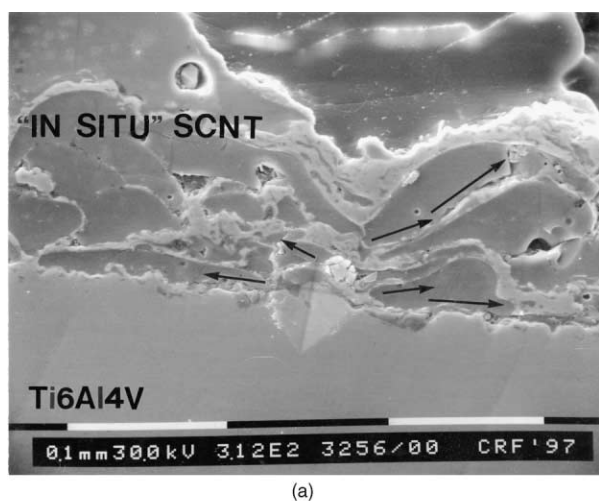
The worse electrochemical behaviour showed by in situ SCNT coated samples in respect to the presintered SCNT coated ones can be attributed to a possible initiation of corrosion due to the poor cohesion degree of the coating. The SEM micrograph of Fig. 9a shows the consequences of the corrosion attack which causes a deep modification of the surface of the samples and the formation of a thick layer of Cl-rich corrosion products, as evidenced by EDS analysis. This phenomenon is less evident on the presintered SCNT coating, as is possible to observe in Fig. 9b: the sample surface, after the an-

odic polarisation test is less affected by the corrosion attack.

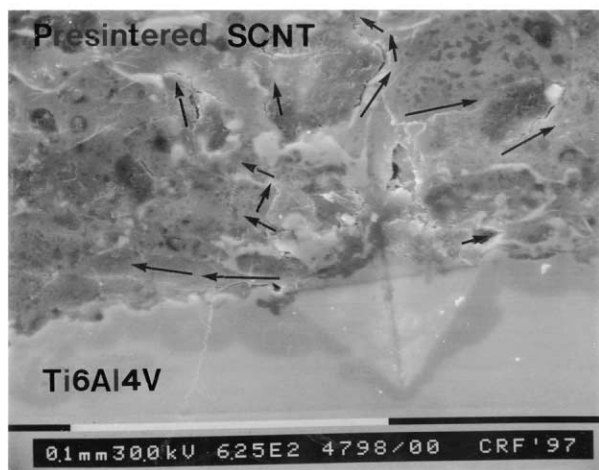
Free corrosion potential (FCP) measurements were carried out in order to evaluate the protective effectiveness of the different coatings toward the substrates. These results confirm the better corrosion behaviour of presintered SCNT coated samples, as evidenced in Fig. 10: although both the curves are characterized by a very similar trend, presintered SCNT coating exhibits FCP values up to 150 mV higher than those of in situ SCNT one. SEM + EDS analysis performed after the electrochemical test revealed the presence of Ca-rich crystals on the surface of the samples (Fig. 11), evidencing a corrosive attack restricted at the glass layer only.<sup>20</sup>

The electrochemical behaviour of TSCBT coatings is quite similar, as evidenced by the anodic polarization curves shown in Fig. 12. In both cases the active-passive transition can be observed, but in situ TSCBT coated samples exhibit a passive current density ( $0.3 \text{ mA/cm}^2$ ) twice with respect to presintered TSCBT coated ones, and a critical passivating current density ( $1 \text{ mA/cm}^2$ ) three times higher. SEM + EDS analysis performed on the samples after the electrochemical test revealed the presence of Cl-rich corrosion products mainly localized at the Ti6Al4V/glass–matrix interface as a consequence of the corrosive attack.<sup>21</sup>

Free corrosion potential (FCP) measurements are in good agreement with the anodic polarization curves. As



(a)



(b)

Fig. 5. Induced crack propagation at the interface between the substrate and (a) the in situ SCNT coating, (b) the presintered SCNT

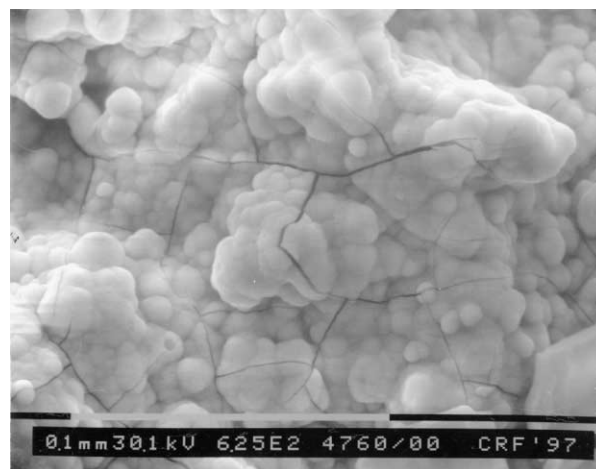


Fig. 6. Plan view of a presintered SCNT composite coating after 30 days soaking in SBF.

Table 4

Shear strength results of the SCN-based coatings

Coating	Shear strength (MPa)
SCN	$26 \pm 7$
In situ SCNT	$26 \pm 16$
Presintered SCNT	$36 \pm 6$

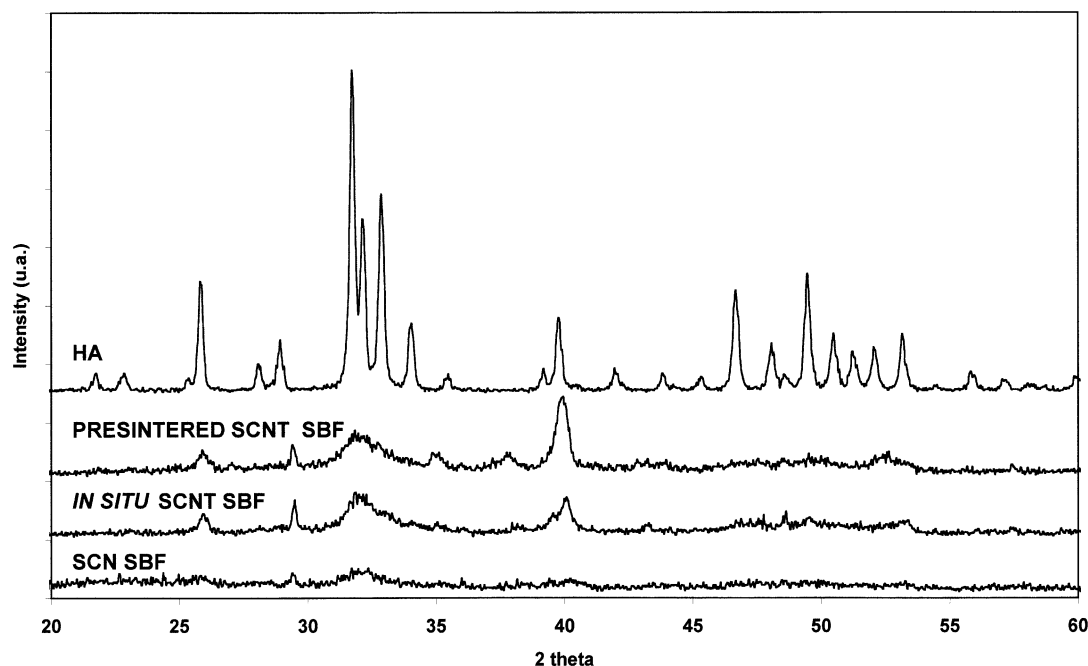


Fig. 7. XRD patterns of the SCN, the in situ SCNT and the presintered SCNT coatings respectively after 30 days soaking in SBF, compared with that of the pure hydroxyapatite.

a matter of fact both the coatings exhibit a similar trend shown in Fig. 13: in the case of in situ TSCBT coated samples the FCP starts from 970 mV(SCE), reaching a constant value of 400 mV(SCE) after 12 h of immersion. For presintered TSCBT coated samples, the FCP decreases from 520 to 640 mV(SCE) within 1 h. After that, it increases slowly, also in this case reaching the constant value of 400 mV(SCE).

#### 4. Conclusions

Glass and composites coatings (SCN, SCNT) were successfully prepared by vacuum plasma spray (VPS) on Ti–6Al–4V substrates. No significant modification of the starting glass–matrix composition was observed during the different steps of the coating preparation. In

order to optimise the composite coatings, the VPS of presintered powdered composites and the in situ plasma spray of a mixture of powdered glass matrix and titanium particles have been compared. The presintered composite coatings were more adherent, dense and homogeneous, and demonstrated a higher shear strength in comparison to the in situ ones. The bioactivity of each kind of coating was demonstrated by in vitro tests.

Anodic polarisation curves and free corrosion potential measurements performed both on the presintered and the in situ composite coatings demonstrated a better electrochemical behaviour of the former in respect of the latter. The corrosion behaviour appears to be mainly influenced by the cohesion degree of the coating.

On the basis of the morphological and mechanical results, it was evident that the sintering process was a useful step for the composites coatings preparation. The best results were always obtained by spraying “composite powders”, i.e. powders formed by Ti particles covered by a layer of glass obtained by milling the presintered composites. Only in this way the softening properties of the glass–matrix were fully used, and a better stability of the interface, both between the glass and the dispersed particles and between the composite coatings and the Ti–6Al–4V substrate, was guaranteed. The in situ method (i.e. the deposition of mixed glass and Ti powders) was not completely satisfactory in terms of homogeneity of the coating, particles distribution, and mechanical properties. The electrochemical behaviour of different coatings prepared by the in situ method and compared with the presintered ones fully confirmed these observations.

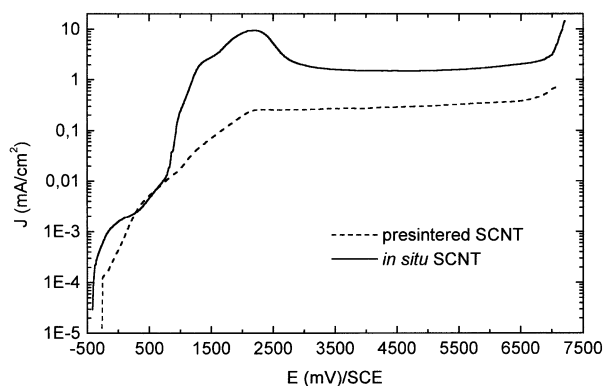
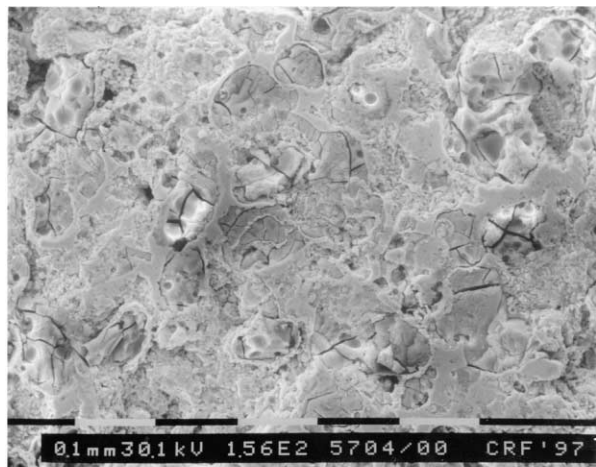
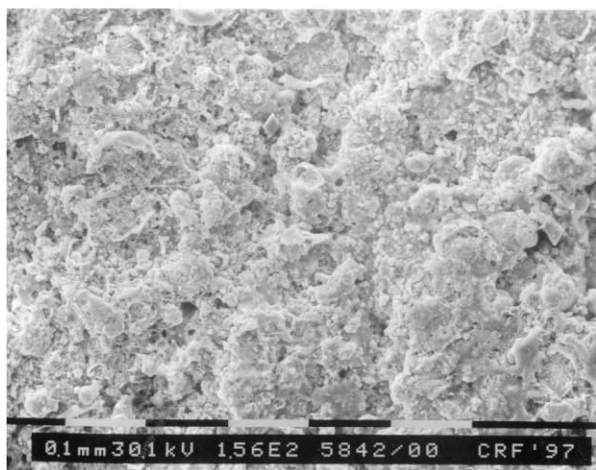


Fig. 8. Anodic polarization curves recorded in Ringer's solution on SCNT coated samples.

We can conclude that, in order to obtain dense and adherent composite coatings with bioactive properties and a good behaviour in contact with biological fluids, the vacuum plasma spray is a valid and reproducible



(a)



(b)

Fig. 9. SEM micrograph of (a) an *in situ* SCNT coated sample surface and (b) of a presintered SCNT coated sample surface after anodic polarization test.

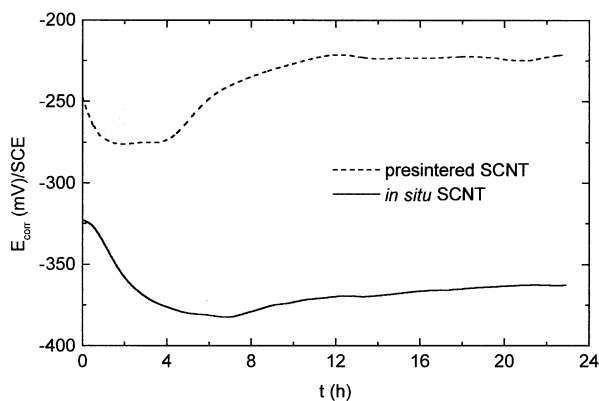


Fig. 10. Free corrosion potential vs. time curves for SCNT coated samples.

technique. In order to guarantee these features great importance is assumed by the powder preparation step, which should provide the formation of composite powders. The sintering process, followed by ball milling of the densified compacts, is a simple and satisfactory method to obtain this kind of starting powders.

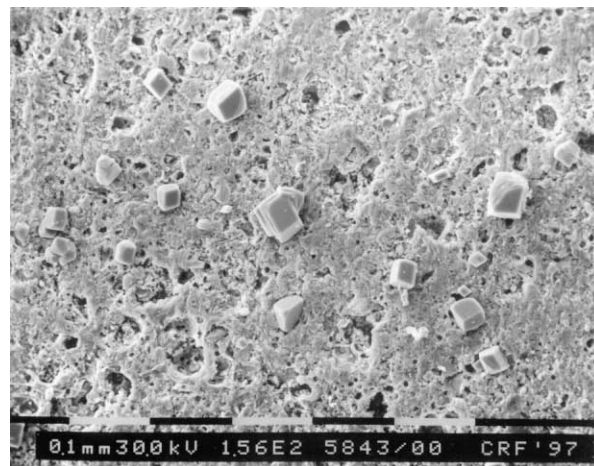


Fig. 11. SEM micrograph of a presintered SCNT composite coated sample surface after free corrosion potential measurements.

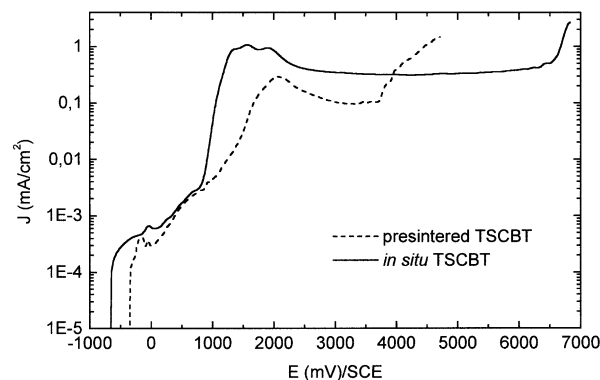


Fig. 12. Anodic polarization curves recorded in Ringer's solution on TSCBT coated samples.

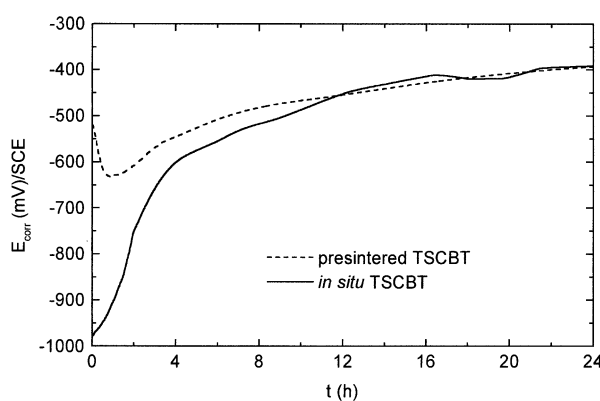


Fig. 13. Free corrosion potential vs. time curves for TSCBT coated samples.



## Acknowledgements

The authors are indebted to the Joint Research Centre of the European Community (Dr. F. Brossa and Ing. L. Paracchini, Ispra, Va, Italy) for VPS facilities, to the Fiat Research Centre (To, Italy) for SEM–EDS analyses, and the “Associazione per lo Sviluppo Scientifico e Tecnologico del Piemonte” (ASP) for financial support. One of the authors (E.V.) wishes to thank Dr. M. Ferraris (Materials Science and Chemical Engineering Department, Politecnico di Torino, Italy) for her helpful discussion and friendly collaboration.

## References

1. Wilson, J., Yli-Urpo, A. and Risto-Pekka, H., Bioactive glasses: clinical applications. In *An Introduction to Bioceramics*, Advances Series in Ceramics, Vol.1 ed. L.L. Hench and J. Wilson., World Scientific Publishing Co., 1993, p. 63.
2. Ohura, K., Nakamura, T., Yamamuro, T., Ebisawa, Y., Kokubo, T., Kotoura, Y. and Oka, M., Bioactivity of CaO–SiO<sub>2</sub> glasses added with various ions. *Journal of Materials Science: Materials in Medicine*, 1992, **3**, 95–100.
3. Verné, E., Ferraris, M. and Jana, C., Pressureless sintering of bioverit®III/Ti particle biocomposites. *J. Eur. Ceram. Soc.*, 1999, **19**, 2039–2047.
4. Ferraris, M., Rabajoli, P., Brossa, F. and Paracchini, L., Vacuum plasma spray deposition of titanium particle/glass-ceramic matrix biocomposites. *Journal of American Ceramic Society*, 1996, **79**(6), 1515–1520.
5. Verné, E., Ferraris, M., Ventrella, A., Krajewski, A. and Ravaglioli, A., Bioactive glass–matrix composite coatings on titanium alloy. In *Ceramic in Oral Surgery*, ed. A. Ravaglioli and A. Krajewski., Gruppo Editoriale Faenza Editrice S.p.A., Faenza, 1995.
6. Ferraris M., Rabajoli P., Verné E., Paracchini L., Chiesa R. and Brossa F. Plasma sprayed biocomposites for clinical applications In: *Materials in Clinical Applications- Advances Science and Technology*, Vol.12, ed. P. Vincenzini, Techna Srl., 1995, p. 281.
7. Verné, E., Terzuolo, A., Mousty, F., Pigozzi, G., Ravaglioli, A., Krajewski, A. and Piancastelli, A., Glass–matrix biocomposite coatings on a Ti–6Al–4V alloy. In *Bioceramics Coatings for Guided Bone Growth*, ed. Ravaglioli, A., Krajewski, A., Gruppo Editoriale Faenza Editrice S.p.A, Faenza, 1997.
8. Verné, E., Ferraris, M., Ventrella, A., Paracchini, L., Krajewski, A. and Ravaglioli, A., Sintering and plasma spray deposition of bioactive glass-matrix composites for medical applications. *Journal of European Ceramic Society*, 1998, **18**(4), 363–372.
9. Gruner, H., *Technical Report*. Plasma Technik, Switzerland, 1986.
10. Kim, H. M., Miyaji, F., Kokubo, T., Ohtsuki, C. and Nakamura, T., Bioactivity of Na<sub>2</sub>O–CaO–SiO<sub>2</sub> Glasses. *Journal of American Ceramic Society*, 1995, **78**(9), 2405–2411.
11. Ferraris, M. and Verné, E., Viscous phase sintering of particle-reinforced glass matrix composites. *J. Eur. Ceram. Soc.*, 1996, **16**, 421–427.
12. Ferraris, M., Salvo, M., Isola, C., Appendino Montorsi, M. and Kohyama, A., Glass-ceramic joining and coating of SiC/SiC for fusion applications. *J. Nucl. Mater.*, 1998, **258–263**, 1546–1550.
13. Isola, C., Salvo, M., Ferraris, M. and Appendino Montorsi, M., Joining of surface modified carbon/carbon composites using a barium-aluminum-boro-silicate glass. *J. Eur. Ceram. Soc.*, 1998, **18**, 1017–1024.
14. Lin, J. and Kato, H., Interfacial Structure and strength of silicon-silicon diffusion bond. *Mater. Sci. Technol.*, 1995, **11**, 1035–1040.
15. Verné, E., Ferraris, M., Moisesescu, C., Ravaglioli, A. and Krajewski, A., Mechanical characterisation of bioactive coatings on zirconia. In *Bioceramics*, Vol. 10, ed. L. Sedel and C. Ray. Paris, France 1997, p. 199.
16. Bushby, R. S. and Scott, V. D., Liquid phase bonding of aluminium and aluminium/nicalon composite using copper interlayers. *Mater. Sci. and Tech.*, 1993, **9**, 417–423.
17. Kokubo, T., Kushitani, H., Ohtsuki, C., Sakka, S. and Yamamuro, T., Chemical Reaction of Bioactive Glass and Glass-ceramics with a Simulated Body Fluid. *J. Mater. Sci. : Mat. Med.*, 1992, **3**, 79–83.
18. Maruno, S., Ban, Y., Wan, H. and Iwata, H. Itoh, Properties of functionally gradient composite consisting of hydroxyapatite containing glass coated titanium and characters for bioactive implant. *J. Ceram. Soc. Jpn. Int. Ed.*, 1992, **100**, 372–377.
19. Sbaizero, O. and Lucchini, E., Influence of residual stresses on the mechanical properties of a layered ceramic composite. *J. Eur. Ceram. Soc.*, 1996, **16**, 813–818.
20. Chen Lin, J. H., Chen, C. P. and Ju, K. S., Biocorrosion behavior of hydroxyapatite/bioactive glass plasma sprayed on Ti6Al4V. *Mater. Chem. Phys.*, 1995, **41**, 282–289.
21. Sousa, S. R. and Barbosa, M. A., Effect of hydroxyapatite thickness on metal ion release from Ti6Al4V substrates. *Biomaterials*, 1996, **17**, 397–404.